

The determination of shock ramp width using the noncoplanar magnetic field component

J. A. Newbury and C. T. Russell

Institute of Geophysics and Planetary Physics and the Department of Earth and Space Sciences, University of California Los Angeles

M. Gedalin

Department of Physics, Ben-Gurion University, Beer-Sheva, Israel

Abstract. We determine a simple expression for the ramp width of a collisionless fast shock, based upon the relationship between the noncoplanar and main magnetic field components. By comparing this predicted width with that measured during an observation of a shock, the shock velocity can be determined from a single spacecraft. For a range of low-Mach, low- β bow shock observations made by the ISEE-1 and -2 spacecraft, ramp widths determined from two-spacecraft comparison and from this noncoplanar component relationship agree within 30%. When two-spacecraft measurements are not available or are inefficient, this technique provides a reasonable estimation of scale size for low-Mach shocks.

Introduction

The determination of spatial scales within the collisionless shock front is one of the central problems for observational shock physics. The width of the shock ramp, defined as the main transition layer between upstream to downstream plasma, is of particular interest. Without spacecraft measurements in a spatial rather than temporal frame of reference, it is impossible to make any comparisons between observations and theoretical models.

For bow shock studies, generally one of two methods has been applied to transform the time series observed by in-situ magnetometers into a spatial magnetic field profile: (1) the comparison of shock observations made by multiple spacecraft with known separations in time and space [for example, *Russell et al.*, 1982; *Farris et al.*, 1993; *Newbury and Russell*, 1996], and (2) the comparison of the temporal duration of the shock foot feature as observed by a single spacecraft with the spatial foot length predicted by a model based on the motion of specularly reflected ions [for example, *Scopke et al.*, 1983; *Gosling and Thomsen*, 1985; *Newbury and Russell*, 1996]. Both methods assume that the bow shock is stationary and one-dimensional, and each has its own limitations. The first is not reliable when the time delay between spacecraft observations is too large [*Newbury and Russell*, 1996] (non-stationarity can affect the results) or too small (relative

errors become large). Also, large transverse spatial separations of the spacecraft with respect to the shock front can introduce error due to the three-dimensional nature of the bow shock. The second method is not applicable to laminar shocks (shocks observed during low Mach number and low plasma β conditions). Ion reflection does not play a dominant dissipative role at such shocks, and so there is little or no foot structure available to measure. (In high Mach number shocks, the second method can also be problematic, since the ion reflection is clearly not specular [*Gosling and Thomsen*, 1985; *Gedalin*, 1996c] which affects the model's predictions.)

Because of these limitations, it is desirable to have another independent method for determining shock scale lengths, particularly for laminar shock observations made by a single spacecraft. In this paper, we make use of the noncoplanar component of the magnetic field in the shock ramp in order to estimate a scale size which can in turn be compared with spacecraft observations of low Mach number shocks. In Section 2 we briefly outline the theoretical basis of this method, and then apply the technique to an example of a bow shock observation made by the ISEE spacecraft (Section 3). In Section 4, we examine the results obtained from a variety of low Mach and low β bow shock observations, and find that the proposed method works well, even for shocks which are not strictly laminar.

Theoretical Basis

Within the ramp layer of a fast collisionless shock (such as the Earth's bow shock), the magnetic field is observed to rotate out of the coplanarity plane (the plane defined by the shock normal and the upstream and downstream magnetic field vectors) [Thomsen *et al.*, 1987]. The analytical relation between this noncoplanar component and the main magnetic component of the shock profile was first derived by Jones and Ellison [1987] phenomenologically in an integral form; its approximate nature has been shown observationally by Gosling *et al.* [1988]; Friedman *et al.* [1990]. Recently, Gedalin [1996a] examined the noncoplanar relation using a general two-fluid hydrodynamics approach, and carried out the derivation with only the widely accepted assumptions of shock stationarity, one-dimensionality, and quasi-neutrality. In the coplanarity coordinate system where N denotes the direction along the shock normal, L is along the magnetic field component in the shock plane, and M is directed out of the coplanarity plane, the general expression for the noncoplanar magnetic field component (B_M) is as follows:

$$B_M \left(1 - \frac{B_N^2}{4\pi n m_i v^2}\right) = \frac{c B_N}{4\pi n v e} \frac{d}{dN} B_L - \frac{c}{n v e} \frac{d}{dN} P_{NL}^{(e)} + \frac{B_N}{n m_i v^2} (P_{NM}^{(e)} + P_{NM}^{(i)}) \quad (1)$$

in the limit $m_e \rightarrow 0$, and where n is the number density; v is the N component of the hydrodynamic velocity; $B_N = \text{const}$ and $n v = \text{const}$ (number flux conservation); and P_{ij} are components of the pressure tensor.

It has been shown by Gedalin and Zilbersher [1995] that the appearance of P_{NM} is mainly due to the presence of reflected ions, and that $P_{NM} \ll n_u m_i V_u^2$ for low Mach number shocks [Gedalin, 1996b]. For laminar shocks it is expected [Thomsen *et al.*, 1985] that the relative contribution of the pressure terms is $\sim \beta/M^2$ and therefore the following approximate expression holds:

$$B_M = l_W \frac{dB_L}{dN}, \quad (2)$$

where $l_W = c \cos \theta_{BN} / M \omega_{pi}$ (i.e., $k = 1/l_W$ would be the wavenumber of a whistler, phasestanding upstream of the ramp), θ_{BN} is the angle between the upstream magnetic field and the shock normal, M_A is the Alfvénic Mach number, and c/ω_{pi} is the ion inertial length. It should be emphasized that (2) is a differential analog of the integral relation developed by Jones and Ellison [1987]. However, (2) should be applied only within the ramp where the main contribution $\propto dB_L/dN$ is not small, otherwise the term $\propto P_{NM}$ can dominate.

Therefore, by estimating the slope of the main magnetic field component (dB_L/dt) in the vicinity of the maximum noncoplanar component in an observed shock ramp, one can determine an independent estimate of the velocity of the shock front from (2). It is then straightforward to transform the observed temporal shock profile into a spatial one suitable for comparison with theory, other shock observations, and/or simulations. An advantage of the method outlined above is that it gives the scale in the relative physical units and not absolute units. It encounters, however, the same difficulties from the determination of the vector basis (N, M, L), as all other methods.

Further difficulties can arise from (2) since it is sensitive to gradients in the field profile; noise and wave activity associated with an observation of a bow shock can make the measurement of dB_L/dt difficult, and traditional filtering techniques do not preserve gradients well. For laminar shocks, a simple variation of the method approximates the shock ramp profile with a hyperbolic tangent function along the N direction:

$$B_L = \frac{B_u + B_d}{2} + \frac{B_d - B_u}{2} \tanh \frac{3N}{l_r}, \quad (3)$$

where B_u and B_d refer to the total field upstream and downstream of the shock front, and the coefficient 3 ensures that 90% of the magnetic field variation occurs within the ramp, $-l_r/2 < N < l_r/2$. In this case, from (2) one immediately has an expression for the ramp width:

$$l_r = 1.5 l_W \frac{B_d - B_u}{B_{M,\max}}. \quad (4)$$

This approach requires accurate measurements of B_u and B_d , but is less sensitive to the local B_L gradient than the direct application of (2) to an observed shock profile.

A Sample Bow Shock

In the present section we apply the proposed method to a quasi-perpendicular collisionless shock crossing that was observed by the ISEE-1 and -2 spacecraft on November 26, 1977, 06:10 UT. The magnetic profile of this shock was measured by the ISEE-1 and -2 UCLA fluxgate magnetometers [Russell, 1978]. Data is filtered to obey the Nyquist criterion and then sampled at the rate of 16 vectors per second. By averaging over a minute of data upstream and downstream of the shock front and applying the coplanarity theorem, the shock normal is determined, and the angle between the shock normal and the upstream magnetic field is found to be $\theta_{BN} = 67^\circ$. Figure 1 shows the high-resolution ISEE-1 observation of total magnetic field and its three components (B_N, B_M, B_L), rotated into coplanar coordinates.

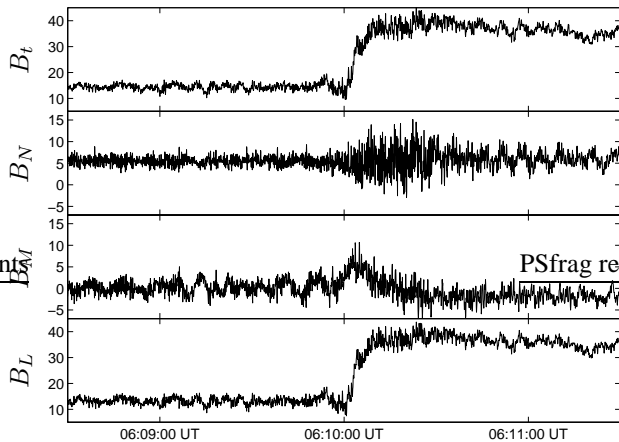


Figure 1. The magnetic profile in the coplanar frame for a laminar shock observed by ISEE-1 on November 26, 1977. $M_A = 2.7$, $\beta = 0.52$, and $\theta_{BN} = 67.0^\circ$.

Plasma measurements of the upstream solar wind are obtained from the ISEE-1 and ISEE-3 solar wind experiments [Bame *et al.*, 1978], and are used to calculate the following parameters: ion inertial length, $c/\omega_{pi} = 58$ km; the Alfvénic Mach number $M_A = 2.7$ (so that $l_W = 8.3$ km); and electron and ion beta, $\beta_e = 0.36$ and $\beta_i = 0.16$, respectively.

In order to remove short wavelength noise while maintaining the gradients within the shock profile, the data was denoised applying a discrete wavelet transform [see, for example, Chui, 1992; Donoho, 1993] (using the Daubechies-10 wavelet) and removing the 6 finest scales. This approximately corresponds to the removal of scales shorter than $2^6 = 64$ data points, which in turn roughly corresponds to 4 second averaging for this 1/16 sec. resolution observation. Although substantial oscillations persist in the upstream and downstream regions, the behavior of B_M and B_L within the ramp is consistent with the theoretical prediction, as seen in Figure 2.

Comparison of $B_{M,\max}$ with the slope of B_L gives the following shock velocity estimate from the noncoplanarity: $V_{sh} = 4.4$ km/s. Independently, the shock velocity estimated from the ISEE-1 and ISEE-2 spacecraft separation is $V_{sh} = 5.7$ km/s (separation $L_s = 20$ km along the shock normal and ramp crossing time separation of 3.5 s). The two estimates agree within 50% deviation.

Applying the hyperbolic tangent approximation from equation (3), the ramp width is estimated to be 47.72 ± 7.5 km. Measuring the ramp based upon two-spacecraft comparisons, ramp width is found to be 56.7 ± 8.2 km. (The temporal duration of the ISEE-1 ramp observation

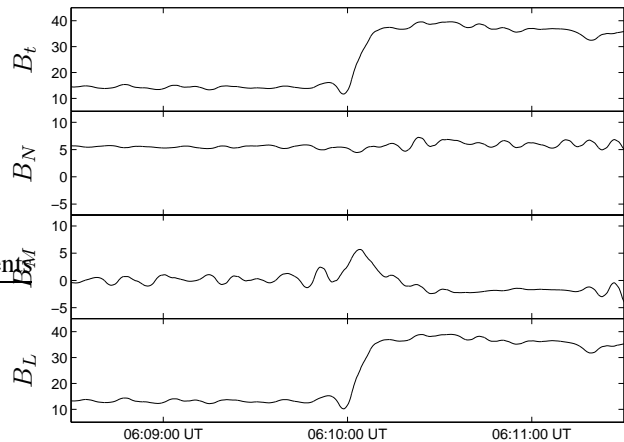


Figure 2. The magnetic profile of the shock, with short period noise removed using a wavelet filter (Daubechies, 10 wavelet with the 6 finest scales removed).

is approximately 10.25 sec.) Uncertainty in both calculations is primarily dominated by the uncertainty in the shock normal determination (which is in turn a result in deviations from the upstream and downstream field measurements). These two estimations of ramp width agree within 20%.

Application to a Variety of Shocks

In order to estimate the reliability of the method outlined in the previous section, we compare the results of the proposed approach from a variety of low-Mach number shock observations. Table 1 contains relevant parameters for a selection of shocks observed by the ISEE spacecraft: the Alfvénic Mach number (M_A), ratio of criticality (R_c), θ_{BN} (as determined by coplanarity), total β of the upstream plasma, the variation of the normal component of the magnetic field during the observation of the shock ramp (normalized by the maximum noncoplanar component in the ramp, $\Delta B_N/B_{M,\max}$), and the results from estimating ramp width using equation (3) ($l_{r,\text{pred}}$) and from the comparison of the ISEE observations ($l_{r,\text{obs}}$). These shocks were selected for their low- β , low-Mach number, quasi-perpendicular ($\theta_{BN} > 45^\circ$) characteristics, as well as being observed at times when the ISEE-1 and -2 spacecraft configurations were ideal for determining fine spatial scales (i.e., small spatial and temporal separations between observations, and θ_{BN} 's calculated by coplanarity and by using an ellipsoidal model of the bow shock agree within 10°). Nearly-perpendicular shocks ($\theta_{BN} > 80^\circ$) are avoided due to the difficulties of determining the shock normal vectors from coplanarity

for such shocks. Also, perpendicular shocks may not have the same whistler mode structure as shocks with lower θ_{BN} [Newbury and Russell, 1996; Friedman et al., 1990]. Many of these shocks have been examined previously by Farris et al. [1993].

For six out of seven shocks, agreement between observations and predictions is very good (within 30%); in comparison, a study of shock velocities based upon two spacecraft observations and on estimations of shock foot length reports agreement within 35% for only half of the shocks examined [Lottermoser and Lühr, 1994]. Also, observation and prediction using the method outlined in this paper are comparable even when the shock is no longer strictly laminar: several of the shocks listed in Table 1 are slightly supercritical (i.e., the ratio of criticality is greater than 1) and are associated with a plasma β that isn't especially low ($\beta > 0.3$).

The shock observed on 79 August 13, 1427 UT is an exception: equation (3) does not accurately estimate its ramp width. This can be explained by considering the effects of turbulence as evidenced in the deviations of the B_N field component within the ramp layer. Equation (2) assumes B_N to remain constant throughout the shock observation, but in reality this is not always so. Two dimensional disturbances and plasma turbulence on the shock front can obscure the coplanarity rotation. Within the shock ramp on 79 Aug. 13, fluctuations of B_N are on the order of $B_{M,max}$, resulting in an under-estimated ramp width from (3). Even with the somewhat stringent requirements placed on selecting the shocks listed in Table 1, non-stationarity and turbulence are still a factor which cannot be ignored. In Figure 3, the ratio of observed and predicted ramp widths are compared with the deviation of B_N (normalized to the maximum B_M component). The shock ramps that agree best with the prediction also have the most constant B_N components, and even a noticeable deviation in B_N can still result in a reasonable estimation of ramp width. The light data points in Figure 3 correspond to supercritical shocks ($R_c > 1$).

Conclusions

We have examined the relationship between the non-coplanar component and gradient of the main component of the magnetic field within the collisionless shock ramp layer. By estimating the scale size of the ramp width based upon this relationship and comparing that length with the temporal duration of a shock ramp observation, the velocity of the shock speed in the spacecraft frame can be calculated. The observed temporal shock profile can then be transformed into a spatial frame, suitable for compari-

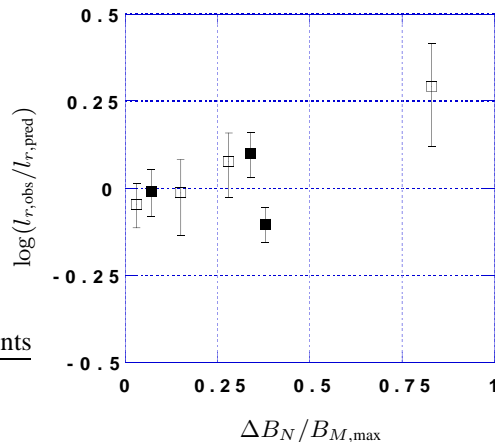


Figure 3. The agreement between observation and prediction of ramp width vs. the deviation of the normal magnetic field component within the ramp observation. When B_N remains constant throughout the shock ramp, the prediction of ramp width is the most accurate. Open squares indicate supercritical shocks.

son with other shock observations and with theory. Based upon a sampling of bow shock observations made by the ISEE-1 and -2 spacecraft, we conclude that this technique is a satisfactory alternative when two-spacecraft comparisons are not feasible, provided that Mach number and plasma β are low (although not strictly laminar) and the rotation of the shock profile into the coplanarity plane is fairly clean.

Acknowledgments. The wavelet transform has been done using WaveLab package for Matlab. Magnetic field plots has been produced using Matlab. This research was supported by grant 94-00047 from the United States-Israel Binational Science Foundation (BSF), Jerusalem, Israel.

References

- Bame, S.J., J.R. Asbridge, H.E. Felthaus, J.P. Glore, G. Paschmann, P. Hemmerich, K. Lehmann, and H. Rosenbauer, ISEE-1 and ISEE-2 fast plasma experiment and the ISEE-1 solar wind experiment, *IEEE Trans., GE-16*, 216, 1978.
- Chui, C.K., *Introduction to Wavelets*, Academic Press, San Diego, 1992.
- Donoho, D., Nonlinear wavelet methods for recovery of signals, densities, and spectra from indirect and noisy data, *Different Perspectives on Wavelets, Proceedings of Symposia in Applied Mathematics*, Vol. 47, I. Daubechies ed. Amer. Math. Soc., Providence, R.I., 1993, pp. 173-205.
- Farris, M.H., C.T. Russell, and M.F. Thomsen, Magnetic structure of the low beta, quasi-perpendicular shock, *J. Geophys. Res.*, 98, 15285, 1993.
- Friedman, M.A., C.T. Russell, J.T. Gosling, and M.F. Thomsen, Noncoplanar component of the magnetic field at low Mach number shocks, *J. Geophys. Res.*, 95, 2441, 1990.
- Gedalin, M., Noncoplanar magnetic field and cross-shock potential in collisionless shock front, *J. Geophys. Res.*, 101, 11153, 1996a.
- Gedalin, M., Transmitted ions and ion heating in nearly-perpendicular low-Mach number shocks, *J. Geophys. Res.*, 101, 15569, 1996b.
- Gedalin, M., Ion reflection at the shock front revisited, *J. Geophys. Res.*, 101, 4871, 1996c.
- Gedalin, M., and D. Zilbersher, Non-diagonal ion pressure in nearly-perpendicular collisionless shocks, *Geophys. Res. Lett.*, 22, 3279, 1995.
- Gosling, J.T. and M.F. Thomsen, Specularly reflected ions, shock foot thicknesses, and shock velocity determinations in space, *Geophys. Res. Lett.*, 90, 9893, 1985.
- Gosling, J.T., D. Winske, and M.F. Thomsen, Noncoplanar magnetic fields at collisionless shocks: A test of a new approach, *J. Geophys. Res.*, 93, 2735, 1988.
- Jones, F.C., and D.C. Ellison, Noncoplanar magnetic fields, shock potentials, and ion deflection, *J. Geophys. Res.*, 92, 11205, 1987.
- Lottermoser, R.-F., and H. Lühr, Estimating the bow shock normal speed from single spacecraft observations of magnetic wave activity, *Geophys. Res. Lett.*, 21, 2055, 1994.
- Newbury, J.A. and C.T. Russell, C.T., Observations of a very thin collisionless shock, *Geophys. Res. Lett.*, 23, 781-784, 1996.
- Russell, C.T., The ISEE 1 and 2 fluxgate magnetometers, *IEEE Trans., GE-16*, 239, 1978.
- Russell, C.T., M.M. Hoppe, W.A. Livesey, J.T. Gosling and S.J. Bame, ISEE-1 and -2 observations of laminar bow shocks: Velocity and thickness, *Geophys. Res. Lett.*, 9, 1171-1174, 1982.
- Sckopke, N., G. Paschmann, S.J. Bame, J.T. Gosling, and C.T. Russell, Evolution of ion distributions across the nearly perpendicular bow shock: Specularly and nonspecularly reflected-gyrating ions, *J. Geophys. Res.*, 88, 6121, 1983.
- Thomsen, M.F., J.T. Gosling, S.J. Bame, and M.M. Mellott, Ion and electron heating at collisionless shocks near the critical Mach number, *J. Geophys. Res.*, 90, 137, 1985.
- Thomsen, M.F., J.T. Gosling, S. J. Bame, K.B. Quest, D. Winske, W. A. Livesey, and C.T. Russell, On the noncoplanarity of the magnetic field within a fast collisionless shock, *J. Geophys. Res.*, 92, 2305, 1987.
- M. Gedalin, Department of Physics, Ben-Gurion University, P.O. Box 653, Beer-Sheva 84105, Israel. (e-mail: gedalin@bgumail.bgu.ac.il); J. A. Newbury and C. T. Russell, IGPP/UCLA, 405 Hilgard Ave., Los Angeles, CA 90095-1567 (e-mail: newbury@igpp.ucla.edu, ctrussell@igpp.ucla.edu)

This preprint was prepared with AGU's L^AT_EX macros v4. File width formatted August 12, 2018.

With the extension package 'AGU++', version 1.3 from 1995/12/01

Table 1. Shock Parameters, Normal Component
Variation in the Ramp, and Ramp Width Calculations

Date	M_A	R_c	θ_{BN}	β	$\frac{\Delta B_N}{B_{M,\max}}$	$l_{r,\text{pred}}$ [km]	$l_{r,\text{obs}}$ [km]	$l_{r,\text{obs}}/l_{r,\text{pred}}$
77 Nov 26, 0610 UT	2.73	1.16	67.0°	0.52	0.28	47.7 ± 7.5	56.7 ± 8.2	1.19 ± 0.25
77 Nov 26, 0619 UT	3.07	1.32	69.3°	0.62	0.15	52.3 ± 9.1	50.6 ± 8.6	0.97 ± 0.24
78 Aug 27, 2007 UT	2.23	0.85	74.6°	0.16	0.38	127 ± 12	100.3 ± 5.6	0.790 ± 0.09
79 Aug 13, 1427 UT	3.75	1.4	78.7°	0.10	0.83	34 ± 11	66.7 ± 2.4	1.96 ± 0.64
79 Sep 18, 1029 UT	2.92	1.15	62.3°	0.18	0.03	92 ± 13	83.2 ± 1.5	0.90 ± 0.13
80 Sep 6, 1006 UT	2.44	0.98	61.6°	0.17	0.34	71.5 ± 9.3	90.0 ± 6.6	1.26 ± 0.19
80 Dec 19, 1435 UT	1.67	0.62	74.8°	0.04	0.07	102 ± 15	100.0 ± 5.8	0.98 ± 0.15